

Monitoring and simulation of hydrothermal conditions indicating the deteriorating stability of a perennially frozen moraine dam in the Himalayas

XIN WANG,^{1,3} CHENGDE YANG,¹ YANLIN ZHANG,¹ KAILGUO CHAI,¹ SHIYIN LIU,² YONGJIAN DING,³ JUNFENG WEI,¹ YONG ZHANG,¹ YONGSHUN HAN¹

¹School of Resource, Environment and Safety Engineering, Hunan University of Science and Technology, Xiangtan, China

²Institute of International Rivers and Eco-security, Yunnan University, Kunming, China

³State Key Laboratory of Cryospheric Science, Northwest Institute of Eco-Environment and Resources, Chinese Academy of Sciences, Lanzhou, China

Correspondence: Xin Wang <xinwang_hn@163.com>

ABSTRACT. Thermal and hydrological dynamics and their impacts on the stability of a moraine dam were analyzed and simulated for the Longbasaba Lake in the Himalaya, based on soil temperature, moisture and heat flux data observed at different depths in the dam from 2012 to 2016. Annual average heat income is greater than heat expenditure on the dam surface. The mean annual temperature at observed the depths of 0–150 cm is $>0^{\circ}\text{C}$, although the average annual air temperature was -3.6°C over the dam, indicating a relatively larger temperature difference between moraine dam and air. The volumetric soil moisture content is relatively low with an annual average of 5%, peaking after the snow cover melting and active layer thawing. Simulation results indicate that the average yearly maximum thawing depth has been ~ 0.3 m deeper than the average yearly maximum freezing depth during the observation period. In the past 55 years, the yearly maximum thawing depth has increased, while yearly maximum freezing depth has decreased, implying that the permafrost in the dam has been deteriorating. The annual surplus heat and increasing permafrost thawing depth will result in further deterioration of permafrost and melting of buried ice in the dam, thereby decreasing its stability.

KEYWORDS: glacier stability, hydrothermal state, moraine dam

1. INTRODUCTION

The lower limit of permafrost elevation on the northern slope of the Himalaya is generally considered as 5100–5300 a.s.l. (Cheng and Wang, 1982; Gruber, 2012; Zou and others, 2017). Above the lower limit, there are thousands of moraine-dammed lakes (Nie and others, 2013; Wang and others, 2014a; Zhang and others, 2015). These moraine dams are generally composed of poorly sorted sediment, frozen soil, and buried ice. Changes in the hydraulic and thermal states within a dam, which are the key parameters for assessing the dam stability and probability of moraine-dammed lake outburst flood (Wang and others, 2012), are closely related to the ground freezing and thawing processes. It has been reported that the permafrost has been gradually degrading in the Tibetan Plateau (TP) during the past decades, and it is presumed that this degradation will continue or accelerate in the coming decades (Wu and Zhang, 2008, 2010; Zhang and Wu, 2012; Wang and others, 2014b). At global scale, this degradation can affect climate (Cheng and Wu, 2007), lake volume changes (Li and others, 2014; Zhang and others, 2017), hydrology and water resources (Woo and others, 2008; Niu and others, 2010), slope stability (Gruber and Haeberli, 2007; Gruber and others, 2016; Haeberli and others, 2016), ecology and engineering projects (Yang and others, 2010; Wu and Niu, 2013) in the TP. Many models have been developed for simulating the ground freezing and thawing processes over the last decades, and they are frequently used to reproduce the historical behavior of permafrost and forecast future

changes of frozen ground and associated impacts on relevant processes, e.g. permafrost stability (Riseborough and others, 2008; Wang and others, 2017). Permafrost degradation has led to decreased stability and changes in the internal structure of moraine dams. Melting of buried ice within a moraine dam can reduce the height of the freeboard and make the seepage increase (Richardson and Reynolds, 2000a, b). Thawing permafrost in a moraine dam can weaken the dam, which will cause these dams to fail more easily if they are overtopped by a displacement wave or offer less resistance to outflow erosion (Balmforth and others, 2008; Westoby and others, 2014). Therefore, in the context of general permafrost degradation and increasingly serious threats of glacial lake outburst floods (GLOFs) in the TP, it is of great practical significance to analyze the states of water and heat in the moraine dams and associated impacts on the dam stability.

Studies of the typical glacial lake moraine dams have mainly focused on the qualitative assessments of dam stability and hazard risk of GLOFs with respect to geometry and internal structure (e.g. ice cores or interstitial ice) (McKillop and Clague, 2007; Wang and others, 2012). It is usual to use a ratio of moraine width to height to describe the shape of a moraine dam, i.e. the smaller the ratio, the higher the likelihood of moraine-dammed lake failure (Huggel and others, 2004; Wang and others, 2012; Rounce and others, 2016). Fujita and others (2013) developed a dam geometry parameter to indicate the potential danger of a moraine-dammed lake. The proposed parameter, the steep lakefront

area, on which a depression angle is steeper than the threshold of 10° , can describe the stability of a dam and its capacity to resist hydrostatic pressure. Buried ice is one of the most important factors for assessing the stability and susceptibility of a moraine dam to failure. For example, accelerated melting of buried ice will damage the integrity of a dam and subsequently compromise its ability to resist the hydrostatic pressure, expand the piping/seepage flow and reduce the freeboard (Clague and Evans, 2000; Emmer and Cochachin, 2013). Although geophysical soundings (seismic refraction, geoelectrical resistivity, gravimetry, radio-echo sounding) have been used to determine the inner structure of ice-cored moraine dams (Richardson and Reynolds, 2000a; Haerberli and others, 2001; Janský and others, 2009; Moore and others, 2011), most current work has focused on GLOFs hazard identification from remote sensing by defining the geometry and topographic/morphological environment of dams, the geometrical shape of the dam or changes in the permafrost of the dam. It was consistently reported that buried ice within a dam increased its susceptibility to failure (Huggel and others, 2004; McKillop and Clague, 2007; Bolch and others, 2011; Wang and others, 2012; Rounce and others, 2016).

However, in a permafrost area, the ability of moraine dams with similar geometric shape and internal structure to resist hydrostatic pressure, seepage- or piping-induced failure may be different, due to changing hydrothermal status (Haerberli and others, 2001; Wang and others, 2012). Monitoring and simulating variations in hydrothermal regimes within a dam are foundational to a further assessment of dam stability. Because moraine dams are often found in remote alpine areas, field surveys of moraine

dams are difficult and, to date, there are few studies focusing on their changing hydrothermal states. In this study, we present the hydrothermal states within the active layer of a perennially frozen moraine dam and analyze the aspects of the related dam stability at Longbasaba Lake on the north side of the Himalaya, based on in situ observation from 2012 to 2016.

2. STUDY AREA

The moraine-dammed Longbasaba Lake ($27^\circ57'17''\text{N}$, $88^\circ04'55''\text{E}$, 5520 m a.s.l.) is located at the source of the Pumqu River watershed in the northern Himalaya (Fig. 1a). Annual average air temperature is -3.6°C and average humidity is 40%. The morphology of the dam exhibits the features of viscous flow in ice-rich sediments and thermo-karst features (Fig. 1b). The lake is 2210 m long from south to north and 685 m wide from east to west with an average depth of 47.5 m and a total water volume of $6.4 \times 10^7 \text{ m}^3$ (Yao and others, 2012). On the east of the lake, two debris-covered glaciers with ice cracks and serac pillars extend into the lake. The lake area has expanded rapidly during the past decades from 0.33 km^2 in 1977 to 1.43 km^2 in 2015 surveyed by aerial photography map and Landsat image. The moraine dam, mainly composed of coarse-grained granite with ice cores, is 163 m wide and 388 m long on average on the top, and 100 m high from bottom to top (Wang and others, 2008). There are many depressions in the moraine dam where several small ponds have developed (Fig. 1b). The outlet flow continues laterally eroding the moraine dams. Longbasaba Lake is reported to have a very high probability of dam failure (Wang and others,

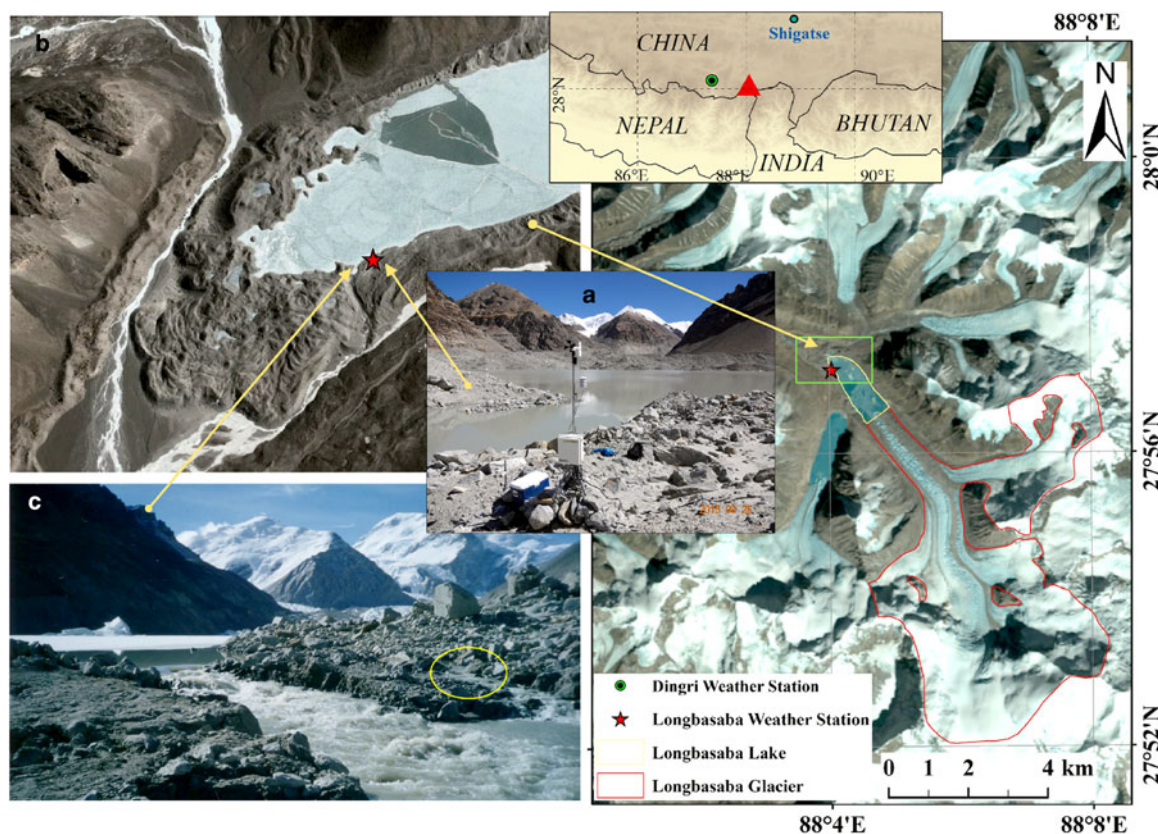


Fig. 1. Map showing the location of Longbasaba Lake and Dingri Weather Station. (a) Observation site and Automatic Weather Station on the moraine dam at Longbasaba Lake, (b) landscape of the moraine dam (Google earth image, January, 2017), (c) overtopping flow and seepage flow of the Longbasaba Lake moraine dam (the outlet of seepage flow marked by yellow circle).

2012). If the dam fails under the 'worst-case' scenario, peak discharge will reach 1×10^4 to $1 \times 10^5 \text{ m}^3 \text{ s}^{-1}$ at the breach site (Wang and others, 2008).

3. DATA AND METHODOLOGY

An automatic meteorological station was installed to record the air temperature, solar radiation, humidity and other variables on the moraine dam. Two ground heat flux probes (Campbell HFP01SC with an error of $\pm 3\%$) at the depths of 5 and 20 cm; five soil temperature probes (Campbell 109-L with an error of $\pm 0.2^\circ\text{C}$) at the depths of 5, 20, 50, 100 and 150 cm; and four soil moisture probes (Campbell CS616 with an error of $\pm 2.5\%$) at the depths of 5, 20, 50 and 150 cm (Table 1) were installed in the moraine dam near the outlet of Longbasaba Lake to record thermal and hydrological transfer processes from 11 November 2012 to 23 September 2016 (Fig. 1a). All the sensors are connected to a data logger (Campbell CR3000-XT) for automatic recording every 10 min. Additionally, the daily average air temperature was collected from Dingri weather station ($28^\circ 38'$, $87^\circ 05'$, 4300 m a.s.l., Fig. 1) in 1960–2016.

The Stefan equation has been widely implemented in engineering for calculating the freezing or thawing depth in permafrost regions (Jumikis, 1977). This equation is useful for estimating the ground freezing and thawing depths from a small number of parameters (Nelson and others, 1997; Woo and others, 2004; Xie and Gough, 2013). The simplest form of the Stefan equation is:

$$D = \sqrt{\frac{2K \cdot I(t)}{L \cdot \omega \cdot \rho}}, \quad (1)$$

$$I(t) = \int_{t_1}^{t_2} T_s dt, \quad (2)$$

where D is the freezing or thawing depth, K is the thermal conductivity of the soil ($\text{W m}^{-1}\text{C}^{-1}$), L is the mass-based latent heat of fusion for water (J kg^{-1}), ω is the volumetric moisture content (%), ρ is the bulk density of the soil (kg m^{-3}), t is the time, T_s is the soil temperature at a depth of 5 cm ($^\circ\text{C}$) and $I(t)$ is the surface freeze/thaw index. Li and Koike (2003) proposed and evaluated a modified approximation solution for the Stefan equation in a framework of a multilayer system and properly dealt with the influences of

Table 1. Descriptions of the soil hydrothermal state probes used at depths of the moraine dam

Sensor	Model	Accuracy	Measurement range	Company
Temperature probe	109-L	$\sim \pm 0.2^\circ\text{C}$	-50 to $+70^\circ\text{C}$	Campbell Scientific, USA
Water content reflectometer	CS616	$\pm 2.5\%$	0–50% volumetric water content	Campbell Scientific, USA
Heat flux sensors	HFP01SC	$\pm 3\%$	$\pm 2000 \text{ W m}^{-2}$	Campbell Scientific, USA

soil freezing and thawing on the ground thermal conductivity and capacity. In this study, we use the modified approximation Stefan solution to calculate the freezing and thawing processes based on the temperature and water content data observed from different depths in the Longbasaba Lake moraine dam.

To reconstruct the surface temperature of the moraine dam during the period 1960–2012, a linear regression model (soil temperature = $0.72 \times$ air temperature $- 1.86$, $R^2 = 0.88$, $\alpha < 0.001$) is established based on daily mean air temperature data from Dingri station and daily mean soil temperatures at the depth of 5 cm in the moraine dam from 2012 to 2016 (Fig. 2). According to this equation, the daily mean soil temperature at the depth of 5 cm for the moraine dam was extended backwards by daily mean air temperature data from Dingri station for the period 1960–2012 (Fig. 3). Then we simulate the ground freezing and thawing processes over the past 55 years based on the modified Stefan model and the reconstructed data.

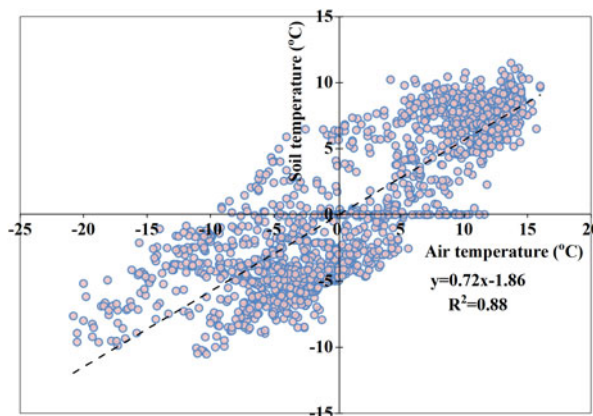


Fig. 2. Relationship between daily mean air temperature from Dingri Weather Station and daily mean soil temperature at the depth of 5 cm in the Longbasaba Lake moraine dam during the period of 2012–2016.

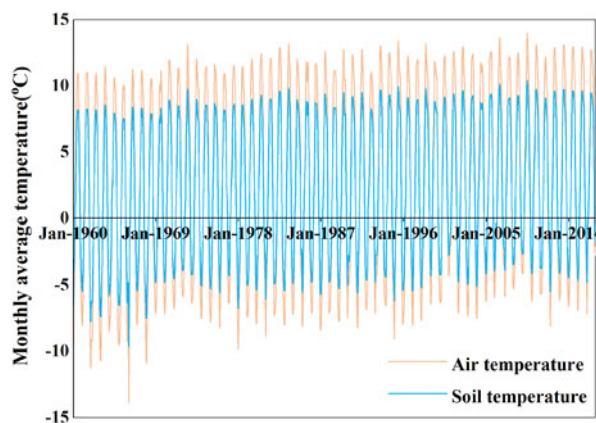


Fig. 3. Variations of air temperature from Dingri Weather Station and the reconstructed soil temperature at the depth of 5 cm in the Longbasaba Lake moraine dam shown by monthly mean temperature in 1960–2016 (the dashed line is the directly measured soil temperatures).

4. RESULTS

4.1. Surface heat flux

The diurnal variation curves for the ground heat flux at the depths of 5 and 20 cm peaked once each year during the study period (Fig. 4a). The minimum monthly mean values at the depths of 5 and 20 cm occurred in January and are -8.5 and -3.9 W m^{-2} , respectively, whereas the maximum monthly mean values occurred in June and are 14.6 and 7.9 W m^{-2} . The ground heat flux was positive during April–September, indicating that heat was transferred from the atmosphere to the soil. From October to the following March it was negative, suggesting that the moraine dam released heat to the atmosphere (Fig. 4b). During the entire observation period, the mean yearly ground heat flux at the depth of 5 cm varied from 0.4 to 1.7 W m^{-2} , with an average value of 1.1 W m^{-2} (Table 2), indicating a yearly surplus of heat transported from the surface into the dam.

4.2. Soil temperature

During the observation period, the mean annual ground temperature of the moraine dam at the depths varied from 0.9°C at 5 cm to 0.5°C at 150 cm, which was higher than the mean annual air temperature over the dam surface (-3.6°C) (Table 2). At the depths of 0–50 cm, the ground temperature was positive during the period May–October and negative from November to the following April. The emergence of positive temperature and the highest soil temperature were gradually retarded with depth. At the depth of 150 cm, the time interval with positive temperatures shifted to June–

December. The 0°C isotherm of ground temperature appeared from the last 10 d of April to the middle of June. The highest ground temperature occurred in July at the dam surface and in September at the depth of 150 cm (Fig. 5). In summer months, the average ground temperature decreased from 5.8°C at 5 cm to 1.9°C at 150 cm, whereas in winter months, the average ground temperature rose from -3.9°C at 5 cm to -1.0°C at 150 cm (Fig. 6).

The vertical ground temperature gradients varied dramatically within the depths from 0 to 20 cm (Fig. 5), with the largest amplitude of variation at the shallowest depth (varied between -0.12 and $+0.13^\circ\text{C cm}^{-1}$). The variation gradually decreased with depth (fluctuating between -0.04 and $+0.06^\circ\text{C cm}^{-1}$ from 20 to 150 cm). The vertical ground temperature gradients were positive in summer (i.e. soil temperature at lower depths was lower than that at upper depths), with the maximum value ($+0.13^\circ\text{C cm}^{-1}$) appearing in June at the depths from 5 to 20 cm. In winter, the gradients were negative (i.e. soil temperature at lower depths was higher than that at upper depths), with the maximum negative value ($-0.12^\circ\text{C cm}^{-1}$) appearing in January at the depths from 5 to 20 cm. On average, the summer, winter and annual mean variation trends of temperature and ground heat flux against depths were largely consistent with each other (Fig. 7).

4.3. Soil moisture

During the observation period, the volumetric soil water content of the moraine dam was relatively low, varying from -2 to 27% (soil humidity data outside the range 0 to

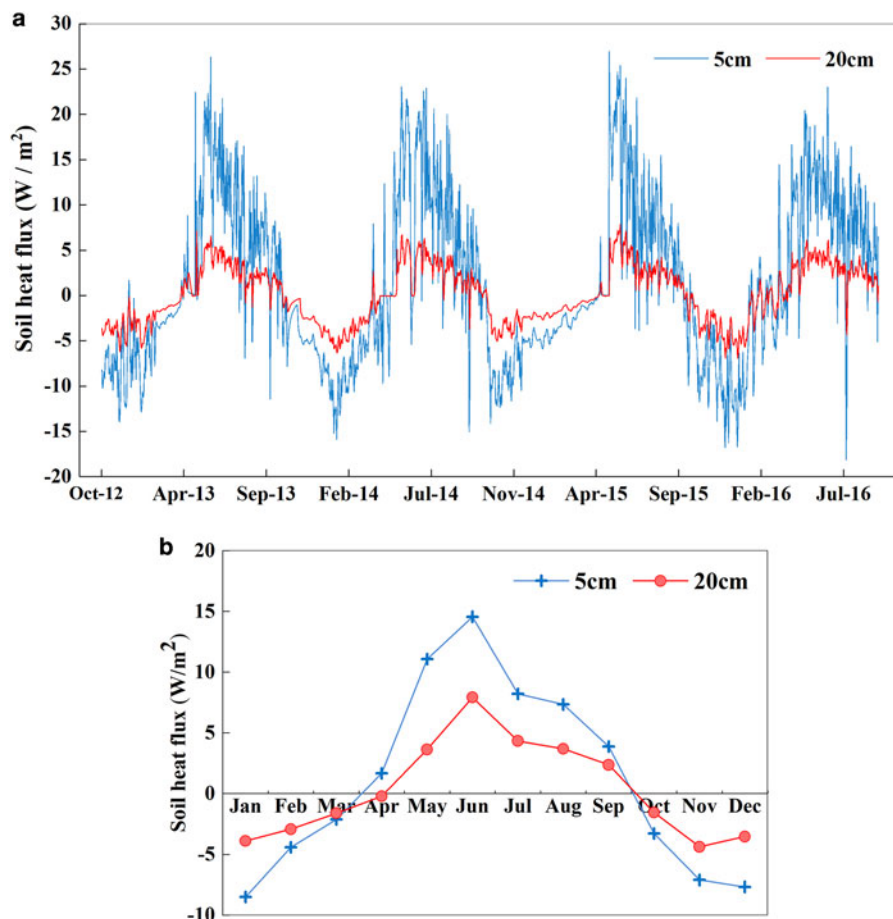


Fig. 4. (a) Diurnal and (b) monthly variations of soil heat flux in the Longbasaba Lake moraine dam from 2012 to 2016.

Table 2. Mean soil temperature, heat flux and moisture of moraine dam at all depths in the time of summer (May to October), winter (November to next April) and annual from 2012 to 2016

Time	Air temperature		5 cm		20 cm		50 cm		100 cm		150 cm	
	Soil temperature	Heat flux Wm^{-2}	Soil moisture %*	Soil temperature	Heat flux Wm^{-2}	Soil moisture %*	Soil temperature	Soil moisture %	Soil temperature	Soil moisture %	Soil temperature	Soil moisture %*
May to October	1.6	5.8	7	4.9	3.4	6	4.5	6	3.1	6	2.1	8
November to next April	-8.4	-3.9	4	-2.9	-2.8	3	-2.5	3	-1.4	3	-0.9	4
Annual	-3.6	0.9	5	0.8	0.3	5	0.8	5	0.7	5	0.5	6

* Soil humidity data outside the range 0 to +70°C were considered invalid according to the manual provided by Campbell Scientific, Inc.

+70°C were considered invalid according to the manual provided by Campbell Scientific, Inc), with an annual average of 5% (Fig. 8). The variations in water content at different depths were largely consistent, as the dam was mainly composed of mixed sand and gravel. The average annual value at the depth of 150 cm (6%) was slightly higher than that at the depths from 5 to 50 cm (5%). The water content at the depths from 5 to 50 cm peaked sharply from the end of April to late May. With the depth increasing, the peak values of water content were delayed and corresponded with the progress of the active thawing front further inside the dam. At the depth of 150 cm, peak water content generally occurred from mid-June to mid-July.

4.4. Freezing and thawing

According to the depth variations of the 0°C isotherm based on observed soil temperatures, the active layer of the moraine dam generally began to thaw in April and the thawing front reached the depth of 150 cm in mid-to-late June. The surface started to freeze in mid-to-late October and froze to the depth of 150 cm in mid-to-late January. The freezing and thawing cycle curves simulated by the modified Stefan model based on the hourly ground temperature and water content at the depth of 5 cm from 2012 to 2016 were similar to the observed ones at the depths of 0–150 cm (Fig. 9). The thawing front reached its maximum depth between 280 and 290 cm in mid-to-late October, and the freezing front reached its maximum depth between 250 and 260 cm in early April to early May (Fig. 9), i.e. the moraine dam reached its yearly maximum freezing depth at the time when frozen soil at the surface began to thaw. The calculated annual maximum thawing depth was 30 cm deeper than the maximum freezing depth on average, which verified that there was an overall surplus of the heat transferred from the surface into the lower dam. The change from freezing to thawing every year occurred in April. Yet, freezing and thawing alternated often in the surface layer of the moraine dam in April due to extreme fluctuations of air temperature and/or the absence of an insulating snow cover.

5 DISCUSSION

5.1. Stratification in the top layer of the moraine dam

Given the continued atmospheric temperature rise, it is to be expected that the diversity of conditions and phenomena encountered in the mountain permafrost exceed what has previously been described and investigated (Noetzli and Gruber, 2009; Gruber and others, 2016). The hydrothermal state of the moraine dam presented evident heterogeneity indicated by the ground heat flux, temperature and moisture content observed at different depths in the dam. In general, the signal of diurnal soil temperature variations can only reach a depth of about 30–50 cm (Hirota and others, 2002). At the depths from 0 to 20 cm, soil temperature fluctuations coincided well with the variations of air temperature. In summer, a diurnal temperature cycle is evident in the depths, characterized by a positive soil temperature gradient (relatively higher temperature at the top than at the bottom) during the day and a negative gradient (relatively lower temperature at the top than at the bottom) at night. The average thawing rate exceeds 3 cm d^{-1} during the

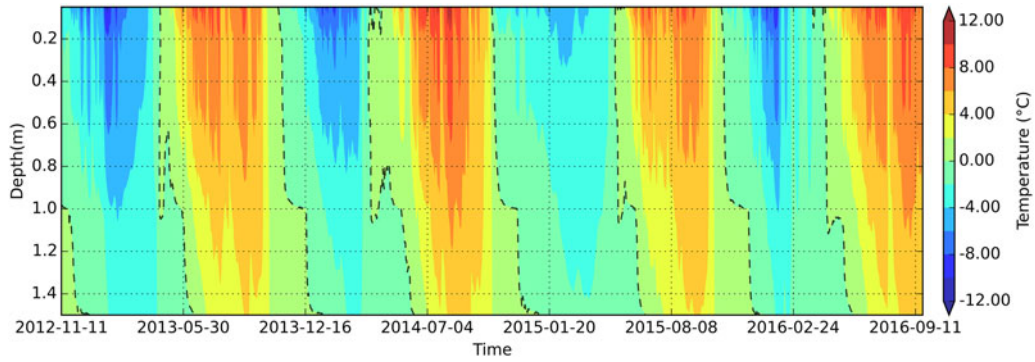


Fig. 5. Diurnal variations of soil temperature in the Longbasaba Lake moraine dam from 2012 to 2016 (the dashed line is 0°C isotherm of soil temperature).

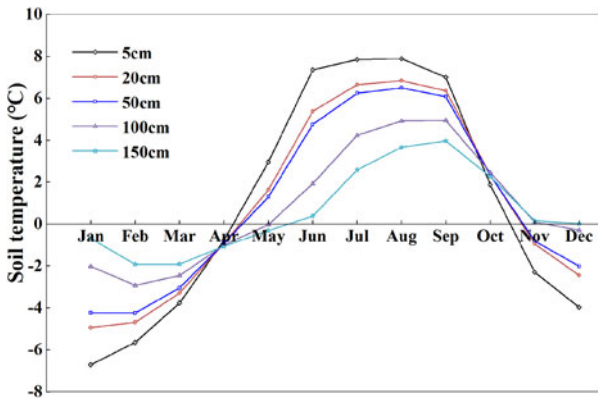


Fig. 6. Monthly mean soil temperature at different depths in the moraine dam of Longbasaba Lake from 2012 to 2016.

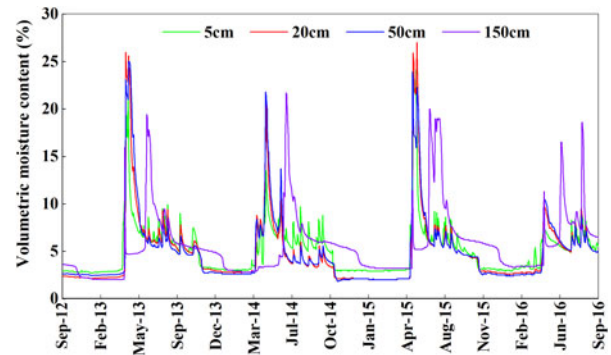


Fig. 8. Daily mean soil moisture variations at different depths in the moraine dam from 2012 to 2016 (soil humidity data outside the range 0 to +70°C were considered invalid according to the manual provided by Campbell Scientific, Inc).

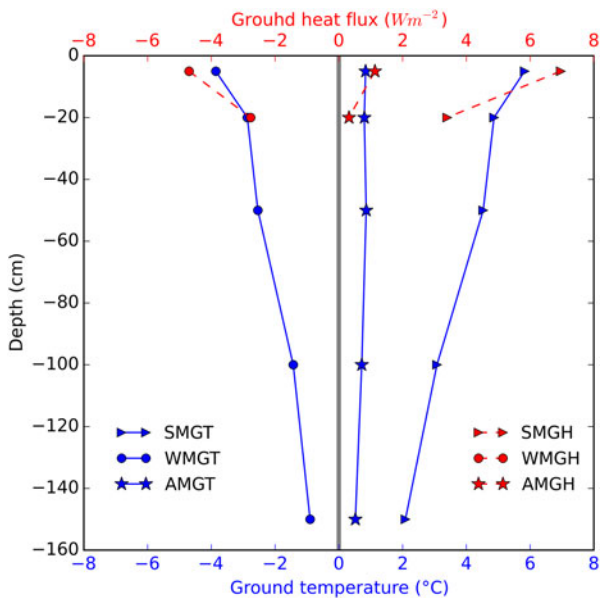


Fig. 7. Profiles of measured mean ground temperature and ground heat flux against different depths in the moraine dam of Longbasaba Lake from 2012 to 2016 (SMGT, summer (May to October) mean ground temperature; WMGT, winter (November to next April) mean ground temperature; AMGT, annual mean ground temperature; SMGH, summer mean ground heat flux; WMGH, winter mean ground heat flux; AMGH, annual mean ground heat flux).

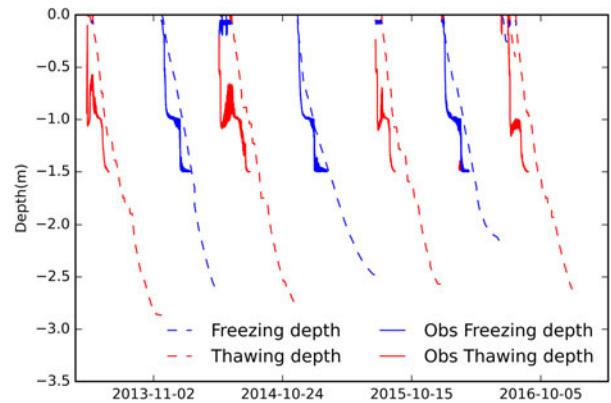


Fig. 9. Comparison of observed (interpolated from soil temperature profiles) and simulated freeze and thaw depths for the Longbasaba Lake moraine dam, from 2012 to 2016.

thawing period. The amplitude of diurnal ground temperature variation was less than that of the air temperature in winter, and vice versa in summer. The energy entering the dam is larger than the amount of energy escaping inferred from an annual average surplus of 1.1 W m^{-2} in the ground heat flux. At the depths from 20 to 100 cm, the diurnal ground temperature cycle gradually disappeared. The amplitude of ground temperature diurnal fluctuations is $<1/5$ to $1/10$ that of air temperature. The thawing rate was

about 2–3 cm d⁻¹ between these depths. At the depths from 100 to 150 cm, the ground temperature was higher than the air temperature and that at other depths in winter, and diurnal variations of ground temperature were almost unobservable. The thawing rate was the smallest (1–2 cm d⁻¹) because the ground heat flux attenuated with increasing depth. Peak moisture content occurs 1–2 months later than at other observed depths as the thawing front moves down over time. Thus, the observed depths of the moraine dam from 0 to 150 cm can be roughly divided into three layers according to the changes in hydrothermal indicators: a surface layer (0–20 cm), a middle layer (20–100 cm) and a deep layer (>100 cm). Relatively small differences were observed in both moisture content and soil temperature within the middle layer, and this could be regarded as a transitional layer between the surface layer and the deep layer of the moraine dam.

The Longbasaba Lake moraine dam is mainly composed of sandy soils and gravels with little difference in terms of material composition at the depths from 0 to 150 cm, indicated by a manually excavated profile. The freezing or thawing, changes of moisture content and layered phenomena of the observed depth in the moraine dam result from differences in hydrothermal exchanges in the processes of water and heat transfer from the dam surface to the interior. The external energy input is a key factor in determining the thermal and hydrological dynamics in the active layer of the dam. Furthermore, the observed stratification is generally dynamic and the depths of surface, middle and deep layers would vary with the changes of water and heat transfer from the dam surface. Additionally, the insulating effect of snow cover reaching to a certain thickness in winter would dampen the ground temperature variations in permafrost (Zhang, 2005; Zhang and others, 2013; Magnin and others, 2017). Similarly, the thick snow cover on the moraine dam would result in a decrease or even disappearance of diurnal soil temperature variations and in the stratification of the moraine dam in winter. For example, an obviously less drastic variation of temperature was recorded in the winter of 2014–2015 possibly indicating a more significant snow cover insulating effect than the other year during 2012–2016 (Fig. 5); the depth of the freezing isotherm remained nearly horizontal but increased gradually from the top to the bottom, suggesting that the stratification of the moraine dam from 0 to 150 cm depth disappeared during this period.

The observed stratification in the Longbasaba Lake moraine dam may affect hydrological processes of the dam. Field investigations showed that overtopping flow occurred in the Longbasaba Lake, which was continually eroding the surface of the moraine dam, and that there was an obvious seepage flow near the outlet (Wang and others, 2008) (Fig. 1c). In the moraine dam, the surface and middle layers (from 0 to 100 cm) are greatly affected by daily air temperature variation and are characterized by a higher thawing rate (>2 cm d⁻¹) in summer. The loose sandy soil and gravels of these two layers are easily eroded by overtopping waves, which will lower or partly lower the freeboard of the lake in summer. For example, an overtopping flood lowered the middle part of the dam near the outlet by 20–30 cm in June and July 2011. From 100 cm to the yearly maximum thawing depth (~290 cm), the dam is in a thawing state from the end of summer to autumn. Piping or seepage flow will likely occur in the deep layer due to the thawed loose sandy soil and gravels overlain by a relatively greater

hydrostatic pressure from the lake water at this time (see-pages were often found below ~1 m from the dam surface from August to October in the investigation period of 2011–2015).

5.2. Changes and implications of freezing/thawing depths

In the coming decades, the main forms of permafrost degradation will be underground ice melting and conversion of low temperature, stable permafrost to warmer permafrost. This process will lead to freezing–thawing disasters related to permafrost changes, such as thaw slumping, frost heaving, thaw subsidence, landslides, destabilization of rock glaciers and frost boils (Lin and others, 2010; Yao and others, 2013; Haeberli and others, 2016; Scotti and others, 2017). Changes in shallow soil temperatures can reflect variations in the thickness of the active layer. It was reported that the annual cumulative temperature at the depth of 50 cm has been rising and the permafrost table has been lowering in the TP over the last decades, leading to more unstable permafrost (Zhao and others, 2011; Li and others, 2012; Wu and others, 2013). Our study site is located in a permafrost area (Cheng and Wang, 1982; Zou and others, 2017) with an elevation of 5520 m a.s.l. The mean annual air temperature increased at a rate of more than 0.03°C a⁻¹ over the period from 1970 to 2010 in this region (Zhang and others, 2012), whereas the nearest meteorological station to the Longbasaba Lake, Dingri station, has recorded a mean annual air temperature increase of 0.062°C a⁻¹ ($\alpha < 0.001$) in the past decades. Under the evidently warming climatic scenario, the Longbasaba Lake area was continuously expanding with an average rate of 0.028 km² a⁻¹ since the 1970s (Yao and others, 2012). Furthermore, air temperature rising in the coming decades will be likely to accelerate the degradation of permafrost (Noetzli and Gruber, 2009) in the dam, which in turn will increase the instability of the dam slope and the possibility of a GLOF (Haeberli and others, 2016).

The ground freezing and thawing processes simulated by the modified Stefan model at the Longbasaba Lake moraine dam indicate that the yearly maximum freezing depth decreased, while the yearly maximum thawing depth increased during 1960–2016 (Fig. 10). Three stages can be identified. (1) From 1960 to 1970, the yearly maximum freezing depth is 0.5 m greater than the yearly maximum thawing depth on average. (2) From 1971 to 1997, there is little difference between the yearly maximum freezing and thawing depths. (3) From 1998 to 2016, the yearly maximum freezing depth is 0.4 m less than the yearly maximum thawing depth on average. Thus, it can be seen clearly that the permafrost in the Longbasaba Lake moraine dam has degenerated over the past 55 years. A layer that is thawing might have developed since the late 1990s in winter, at the depths of about 2.5–2.9 m between the frozen surface and the permafrost, indicating that the permafrost at the dam site is becoming inactive. The corresponding permafrost degradation is likely to affect the internal structure and stability of the dam.

A significant snow cover exists on the dam in winter, reducing the correlation between the ground and air temperatures due to its insulating effects (Haeberli and others, 2010; Staub and Delaloye, 2017). Therefore, the evolution of snow cover would invalidate the linear regression model

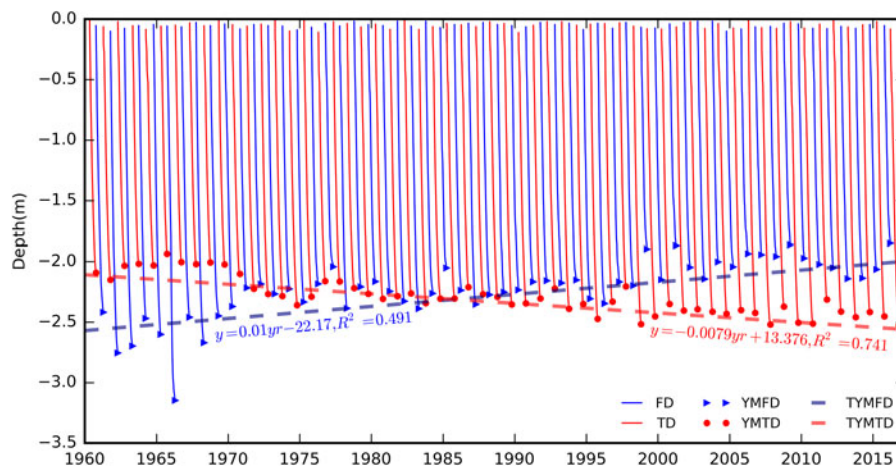


Fig. 10. Freezing and thawing processes of the Longbasaba Lake moraine dam from 1960 to 2016 (FD, freezing depth; TD, thawing depth; YMFD, yearly maximum freezing depth; YMTD, yearly maximum thawing depth; TYMFD, trend of yearly maximum freezing depth; TYMTD, trend of yearly maximum thawing depth).

for reconstructing the surface temperature on the dam and bring errors in the simulation of ground thawing and freezing depths. To delineate the snow insulating effects, a physical-based frozen soil model incorporating a snow cover is necessary. In this study, due to the lack of sufficient data such as precipitation and snow depth on the dam, the relative simple Stefan model was adopted. In addition, the dam site and Dingri station are located in the rain shadow of Mount Everest with low annual and winter precipitation, e.g. about 280 and 5 mm, respectively, at Dingri station. Observations from 1959 to 2016 indicate that there is no significant trend in annual precipitation and winter snow at Dingri. That is, although the snow cover has implications for the ground freezing and thawing depths, it would not significantly change their simulated trends. However, more data will be collected and a physically based model will be used to assess the permafrost evolution of the moraine dam with consideration for factors including snow cover and solar radiation.

The moraine dam failure usually involves the aspects of material strength and permeability, slope stability, piping and/or retrogressive erosion, morphological features and geometric parameters of the dam. The degradation of frozen soil and increased thawing depth are important factors related to decreased moraine dam stability (McKillop and Clague, 2007; Wang and others, 2012), and to slope or dam failure during earthquakes (Kargel and others, 2015). An in situ survey indicated that the dam is composed of unconsolidated and mixed grain-size moraine with high permeability and low shearing resistance. On average, the distal dam flank is steeper than 20° and there is no freeboard (Wang and others, 2008). The outside flank of the moraine dams is being eroded due to more frequent overtopping events (Fig. 1c). The ratio of dam width to height is about 1.6. The dam crest was characterized by striking structures indicating cohesive deformation of ice-rich subsurface material with small lakes indicating thermokarst well developed inside the dam (Fig. 1b). Buried ice covered by debris about 1–3 m thick is exposed in the central part of the inside flank of the moraine. The visible seepages and viscous flow in ice-rich sediments likely enhance the probability of the dam's failure. In conclusion, with the increase of maximum thawing depth in summer and the emergence

of a thawed layer in winter in the interior of the Longbasaba Lake moraine dam, the capacity for water blocking, anti-piping and erosion prevention of the moraine dam would decrease. Meanwhile, melting of buried ice in the dam would be accelerated, which is caused by the annual surplus of heat reaching the inner layers. Such ice melting and thawing of permafrost is likely to produce considerable thaw settlement and surface subsidence at sites with ice-supersaturated materials (excess ice) at depth. Such surface subsidence in the perennially frozen lake dam may affect lake levels, consequently resulting in a further decrease in the stability of the dam body. So far, the hydrothermal state of the frozen moraine dam could only be documented within a shallow surface layer. Important parameters such as the depth of the active layer or the amount and location of buried ice, etc., remain to be investigated and further continuous precision surveying (for instance by drones) would be an important option for continued monitoring at the site.

6 CONCLUSIONS

The annual mean soil temperature was above 0°C at different depths from 0 to 150 cm, although the annual mean air temperature was as low as −3.6°C over the Longbasaba Lake moraine dam from 2012 to 2016. Observed soil moisture content at the dam is relatively lower than that of other investigated sites in TP (Yang and others, 2013) and usually peaked during snowmelt from the end of April to late May. At the depth of 5 cm in the moraine dam, there is an annual surplus of heat transported from the surface to the depths, which may result in permafrost degradation. The seasonal snow cover at the dam surface affects the ground heat flux in winter to some degree due to its insulating effects and further investigations of snow depth and its implication on the dam are needed in future work.

As a result of attenuation of water and heat transfer from the dam surface to the interior, the hydrothermal conditions appear layered at observed depth in the moraine dam. Erosion frequently occurs in the surface and middle layers because they thaw rapidly and suffer from overtopping flow during the entire summer season. Seepage flows most likely occur in the deep layer to the maximum thawing depth (100–290 cm) as the structure is that of a loose,

thawing moraine integrated by a relatively large hydrostatic pressure from lake water at these depths.

The yearly maximum thawing depth (280–290 cm) of the dam occurs from mid-to-late October. The yearly maximum freezing depth (250–260 cm) occurs from the beginning of April to the beginning of May. Over the past 55 years, the yearly maximum thawing depth has been increasing, while the yearly maximum freezing depth has been decreasing, indicating a permafrost degradation in the Longbasaba Lake moraine dam. However, the moraine dam failure usually involves the aspects of material strength and permeability, morphological features and geometric parameters of the dam, and further investigation and more comprehensive analysis are strongly proposed to investigate the deteriorating stability of the moraine dam.

ACKNOWLEDGEMENTS

The authors would like to thank Kunpeng Wu (Northwest Institute of Eco-Environment and Resources, Chinese Academy of Sciences), MSc students Meihai Shu (Hunan University of Science and Technology) and Xiaofeng Li (Northwest Normal University, Lanzhou, China) for their support in fieldwork, and the daily air temperature data (Dingri meteorological station) were obtained freely from the China Meteorological Administration (<http://data.cma.cn/site/index.html>). We thank W. Haerberli and two other anonymous reviewers for insightful comments that improved the manuscript greatly. This study was supported financially by the National Natural Science Foundation of China (grant Nos. 41771075, 41271091 and 41261016) and Fund of State Key Laboratory of Cryosphere Science (SKLCS-OP-2017-05).

REFERENCES

- Balmforth NJ, Hardenberg JV, Provenzale A and Zammett R (2008) Dam breaking by wave-induced erosional incision. *J. Geophys. Res.*, **113**(F1), F01020 (doi: 10.1029/2007JF000756)
- Bolch T and 5 others (2011) Identification of potentially dangerous glacial lakes in the northern Tien Shan. *Nat. Hazards*, **59**(3), 1691–1714 (doi: 10.1007/s11069-011-9860-2)
- Cheng G and Wu T (2007) Responses of permafrost to climate change and their environmental significance, Qinghai-Tibet Plateau. *J. Geophys. Res.*, **112**(F2), F02S03 (doi: 10.1029/2006JF000631)
- Cheng GD and Wang SL (1982) On the zonation of high-altitude permafrost in China. *J. Glaciol. Geocryol.*, **4**(2), 1–17 (in Chinese)
- Clague J and Evans SG (2000) A review of catastrophic drainage of moraine-dammed lakes in British Columbia. *Quat. Sci. Rev.*, **19**(17), 1763–1783 (doi: 10.1016/S0277-3791(00)00090-1)
- Emmer A and Cochachin A (2013) The causes and mechanisms of moraine-dammed lake failures in the Cordillera Blanca, North American Cordillera, and Himalayas. *Acta. Univ. Carol. Geogr.*, **48**(2), 5–15 (doi: 10.14712/23361980.2014.23)
- Fujita K and 6 others (2013) Potential flood volume of Himalayan glacial lakes. *Nat. Hazard Earth Syst.*, **13**(7), 1827–1839 (doi: 10.5194/nhess-13-1827-2013)
- Gruber S (2012) Derivation and analysis of a high-resolution estimate of global permafrost zonation. *Cryosphere*, **6**(1), 221–233 (doi: 10.5194/tc-6-221-2012)
- Gruber S and Haerberli W (2007) Permafrost in steep bedrock slopes and its temperature-related destabilization following climate change. *J. Geophys. Res.*, **112**(F2), F02S18 (doi: 10.1029/2006JF000547)
- Gruber S and 8 others (2016) Review article: inferring permafrost and permafrost thaw in the mountains of the Hindu Kush Himalaya region. *The Cryosphere*, **11**(1), 81–99 (doi: 10.5194/tc-11-81-2017)
- Haerberli W, Käab A, Vonder Mühl D and Teyssie P (2001) Prevention of outburst floods from periglacial lakes at Grubengletscher, Valais, Swiss Alps. *J. Glaciol.*, **47**(156), 111–122 (doi: 10.3189/172756501781832575)
- Haerberli W and 9 others (2010) Mountain permafrost: development and challenges of a young research field. *J. Glaciol.*, **56** (200), 1043–1058 (doi: 10.3189/002214311796406121)
- Haerberli W, Schaub Y and Huggel C (2016) Increasing risks related to landslides from degrading permafrost into new lakes in deglaciating mountain ranges. *Geomorphology* **293**, 405–417 (doi: 10.1016/j.geomorph.2016.02.009)
- Hirota T, Pomeroy J W, Granger R J and Maule C P (2002) An extension of the force-restore method to estimating soil temperature at depth and evaluation for frozen soils under snow. *J. Geophys. Res. Atmos.*, **107**(D24), 4767 (doi: 10.1029/2001JD001280)
- Huggel C, Haerberli W, Käab A, Bieri D and Richardson S (2004) An assessment procedure for glacial hazards in the Swiss Alps. *Can. Geotech. J.*, **41**(6), 1068–1083 (doi: 10.1007/s11069-008-9321-8)
- Janský B and 5 others (2009) The evolution of Petrov lake and moraine dam rupture risk (Tien-Shan, Kyrgyzstan). *Nat. Hazards*, **50**(1), 83–96 (doi: 10.1007/s11069-008-9321-8)
- Jumikis AR (1977) Thermal geotechnics. *Soil Sci.*, **125**(6), 393 (doi: 10.1097/00010694-197806000-00010)
- Kargel JS and 63 others (2015) Geomorphic and geologic controls of geohazards induced by Nepal's 2015 Gorkha earthquake. *Science*, **351**(6269), 140 (doi: 10.1126/science.aac8353)
- Li R and 7 others (2012) Temporal and spatial variations of the active layer along the Qinghai-Tibet highway in a permafrost region. *Chin. Sci. Bull.*, **57**(35), 9–4616 (doi: 10.1007/s11434-012-5323-8)
- Li X and Koike T (2003) Frozen soil parameterization in SiB2 and its validation with GAME-Tibet observations. *Cold Reg. Sci. Technol.*, **36**(1–3), 165–182 (doi: 10.1016/S0165-232X(03)00009-0)
- Li Y, Liao J, Guo H, Liu Z and Shen G (2014) Patterns and potential drivers of dramatic changes in Tibetan lakes, 1972–2010. *PLoS ONE*, **9**(11), e111890 (doi: 10.1371/journal.pone.0111890)
- Lin Z, Niu F, Ge J, Wang P and Dong Y (2010) Variation characteristics of the thawing lake in permafrost regions of the Tibetan Plateau and their influence on the thermal state of permafrost. *J. Glaciol. Geocryol.*, **32**(2), 341–350 (in Chinese) (doi: 1000-0240(2010)02-0341-10)
- Magnin F and 5 others (2017) Snow control on active layer thickness in steep alpine rock walls (Aiguille du Midi, 3842 m a.s.l., Mont Blanc massif). *Catena*, **149**, 648–662 (doi: 10.1016/j.catena.2016.06.006)
- McKillop RJ and Clague JJ (2007) Statistical, remote sensing-based approach for estimating the probability of catastrophic drainage from moraine-dammed lakes in southwestern British Columbia. *Glob. Planet. Change*, **56**(1), 153–171 (doi: 10.1016/j.gloplacha.2006.07.004)
- Moore JR, Boleve A, Sanders JW and Glaser SD (2011) Self-potential investigation of moraine dam seepage. *J. Appl. Geophys.*, **74**(4), 277–286 (doi: 10.1016/j.jappgeo.2011.06.014)
- Nelson F and 5 others (1997) Estimating active-layer thickness over a large region: Kuparuk River basin, Alaska, USA. *Arctic Antarct. Alp. Res.*, **29**(4), 367–378 (doi: 10.2307/1551985)
- Nie Y, Liu Q and Liu S (2013) Glacial lake expansion in the Central Himalayas by Landsat images, 1990–2010. *PLoS ONE*, **8**(12), e83973 (doi: 10.1371/journal.pone.0083973)
- Niu L, Ye BS, Li J and Sheng Y (2010) Effect of permafrost degradation on hydrological processes in typical basins with various permafrost coverage in Western China. *Sci. China Earth Sci.*, **54**(4), 615–624 (doi: 10.1007/s11430-010-4073-1)
- Noetzli J and Gruber S (2009) Transient thermal effects in Alpine permafrost. *Cryosphere*, **3**(1), 85–99 (doi: 10.5194/tc-3-85-2009)
- Richardson SD and Reynolds JM (2000a) Degradation of ice-cored moraine dams: implications for hazard development. In Nakawo M, Raymond CF, Fountain A (Eds), *Debris-covered*

- Glaciers, Proceedings of a Workshop Held at Seattle, Washington, USA, IAHS Publ., 187–198
- Richardson SD and Reynolds JM (2000b) An overview of glacial hazards in the Himalayas. *Quat. Int.*, **65**, 31–47 (doi: 10.1016/s1040-6182(99)00035-x)
- Riseborough D, Shiklomanov N, Etzelmüller B, Gruber S and Marchenko S (2008) Recent advances in permafrost modelling. *Permafrost Periglac.*, **19**(2), 137–156 (doi: 10.1002/ppp.615)
- Rounce DR, McKinney DC, Lala JM, Byers AC and Watson CS (2016) A new remote hazard and risk assessment framework for glacial lakes in the Nepal Himalaya. *Hydrol. Earth Syst. Sci.*, **20**(9), 3455–3475 (doi: 10.1002/ppp.615)
- Scotti R, Crosta GB and Villa A (2017) Destabilisation of creeping permafrost: the Plator Rock Glacier Case Study (Central Italian Alps). *Permafrost Periglac. Process*, **28**, 224–236 (doi: 10.1002/ppp.1917)
- Staub B and Delaloye R (2017) Using near-surface ground temperature data to derive snow insulation and melt indices for mountain permafrost applications. *Permafrost Periglac.*, **28**, 237–248 (doi: 10.1002/ppp.1890)
- Wang C, Jin S and Shi H (2014b) Area change of the frozen ground in China in the next 50 years. *J. Glaciol. Geocryol.*, **36**(1), 1–8 (in Chinese)
- Wang L and 16 others (2017) Development of a land surface model with coupled snow and frozen soil physics. *Water Resour. Res.*, **53**(6), 5085–5103 (doi: 10.1002/2017WR020451)
- Wang W, Xiang Y, Gao Y, Lu A and Yao T (2014a) Rapid expansion of glacial lakes caused by climate and glacier retreat in the Central Himalayas. *Hydrol. Process.*, **29**(6), 859–874 (doi: 10.1002/hyp.10199)
- Wang X, Liu S, Guo W and Xu J (2008) Assessment and simulation for glacier lake outburst flood of Longbasaba and Pida Lakes, China. *Mt. Res. Dev.*, **28**(3), 310–317 (doi: 10.1659/mrd.0894)
- Wang X and 6 others (2012) An approach for estimating the breach probabilities of moraine-dammed lakes in the Chinese Himalayas using remote-sensing data. *Nat. Hazard Earth. Syst.*, **12**(10), 3109–3122 (doi: 10.5194/nhess-12-3109-2012)
- Westoby MJ and 5 others (2014) Reconstructing historic glacial lake outburst floods through numerical modelling and geomorphological assessment: extreme events in the Himalaya. *Earth Surf. Processes Landform*, **39**(12), 1675–1692 (doi: 10.1002/esp.3617)
- Woo MK, Arain MA, Mollinga M and Yi S (2004) A two-directional freeze and thaw algorithm for hydrologic and land surface modelling. *Geophys. Res. Lett.*, **31**(L12501) (doi: 10.1029/2004gl019475)
- Woo MK, Kane DL, Carey SK and Yang D (2008) Progress in permafrost hydrology in the new millennium. *Permafrost Periglac.*, **19**, 237–254 (doi: 10.1029/2004gl019475)
- Wu Q and Zhang T (2008) Recent permafrost warming on the Qinghai-Tibetan Plateau. *J. Geophys. Res.*, **113**(D13), D13108 (doi: 10.1029/2007jd009539)
- Wu Q and Zhang T (2010) Changes in active layer thickness over the Qinghai-Tibetan Plateau from 1995 to 2007. *J. Geophys. Res.*, **115**(D9), D09107 (doi: 10.1029/2009jd012974)
- Wu QB and Niu FJ (2013) Permafrost changes and engineering stability in Qinghai-Xizang Plateau. *Chin. Sci. Bull.*, **58**(10), 1079–1094 (doi: 10.1007/s11434-012-5587-z)
- Xie C and Gough WA (2013) A simple thaw-freeze algorithm for a multi-layered soil using the Stefan equation. *Permafrost Periglac.*, **24**(3), 252–260 (doi: 10.1002/ppp.1770)
- Yang K and 11 others (2013) A multiscale soil moisture and freeze-thaw monitoring network on the third pole. *B Am. Meteorol. Soc.*, **94**(12), 1907–1916 (doi: 10.1175/bams-d-12-00203.1)
- Yang M, Nelson FE, Shiklomanov NI, Guo D and Wan G (2010) Permafrost degradation and its environmental effects on the Tibetan Plateau: a review of recent research. *Earth-Sci. Rev.*, **103**, 31–44 (doi: 10.1016/j.earscirev.2010.07.002)
- Yao TD and 5 others (2013) Cryospheric changes and their impacts on regional water cycle and ecological conditions in the Qinghai-Tibetan Plateau. *Chin. J. Nat.*, **35**(3), 179–186 (in Chinese) (doi: 10.3969/j.issn.0253-9608.2013.03.004)
- Yao X, Liu S, Sun M, Wei J and Guo W (2012) Volume calculation and analysis of the changes in moraine-dammed lakes in the north Himalaya: a case study of Longbasaba lake. *J. Glaciol.*, **58**(210), 753–760 (doi: 10.3189/2012jogG11J048)
- Zhang D, Xiao C and Liu W (2012) Analysis on Himalayan climate change in 1951–2010. *Adv. Clim. Change Res.*, **8**(2), 110–118 (doi: 10.3969/j.issn.1673-1719.2012.02.006) (in Chinese)
- Zhang G, Yao T, Xie H, Wang W and Yang W (2015) An inventory of glacial lakes in the third pole region and their changes in response to global warming. *Glob. Planet Change*, **131**, 148–157 (doi: 10.1016/j.gloplacha.2015.05.013)
- Zhang G and 13 others (2017) Lake volume and groundwater storage variations in Tibetan Plateau's endorheic basin. *Geophys. Res. Lett.*, **44**(11), 5550–5560 (doi: 10.1002/2017GL073773)
- Zhang T (2005) Influence of the seasonal snow cover on the ground thermal regime: an overview. *Rev. Geophys.*, **43**, RG4002 (doi: 10.1029/2004RG000157)
- Zhang W and 7 others (2013) Monitoring and modeling the influence of snow cover and organic soil on the active layer of permafrost on the Tibetan Plateau. *J. Glaciol. Geocryol.*, **35**(3), 528–540 (in Chinese) (doi: 10.7522/j.issn.1000-0240.2013.0062)
- Zhang Z and Wu Q (2012) Predicting changes of active layer thickness on the Qinghai-Tibet Plateau as climate warming. *J. Glaciol. Geocryol.*, **34**(3), 505–511 (in Chinese)
- Zhao L and 5 others (2011) Soil thermal regime in Qinghai-Tibet Plateau and its adjacent regions during 1977–2006. *Adv. Clim. Change Res.*, **7**(5), 307–316 (doi: 10.3969/j.issn.1673-1719.2011.05.001) (in Chinese)
- Zou D and 19 others (2017) A new map of the permafrost distribution on the Tibetan Plateau. *Cryosphere*, **11**(6), 2527–2542 (doi: 10.5194/tc-2016-187)

MS received 10 June 2017 and accepted in revised form 9 April 2018; first published online 2 May 2018